Electronic structure and properties of $CoSi_2$

L. F. Mattheiss and D. R. Hamann
AT&T Bell Laboratories, Murray Hill, New Jersey 07974-2070
(Received 24 December 1987)

The energy-band structure and related electronic properties of cubic $CoSi_2$ have been calculated self-consistently with the use of the linear augmented-plane-wave method. The results are qualitatively similar to those determined previously for $NiSi_2$, assuming a rigid-band adjustment of the Fermi level. The $CoSi_2$ Fermi surface is quite simple, consisting of three nested hole sheets centered at the Brillouin-zone origin. The calculated Fermi-surface dimensions and topology are in excellent agreement with the de Haas–van Alphen data of Newcombe and Lonzarich (preceding paper). The calculated Drude plasma energy and Fermi velocity are combined with the observed resistivity to estimate transport properties such as low-temperature carrier mean free paths ($l \approx 340$ Å). The kinematics of carrier transmission through $Si/CoSi_2$ interfaces and its dependence on interface orientation is analyzed in terms of the projected band structure.

Transition-metal silicides have received increased attention in recent years because of their practical importance in Si device applications.[1] This has been especially true in the case of the cubic disilicides $CoSi_2$ and $NiSi_2$, which both crystallize with the well-known fluorite structure. In both materials, the bulk lattice parameters are close to those of Si. This proves to be favorable for the formation of sharp epitaxial silicon-silicide interfaces which are near perfect at an atomic scale.[2] This has led to detailed studies of their interface properties such as Schottky-barrier heights[3,4] and interface geometry,[3] as well as the fabrication of $Si/CoSi_2/Si$ heterostructures for use as metal-base transistors.[5–9]

These developments have stimulated a parallel interest in the fundamental properties of the bulk silicide materials. For example, photoemission[10–12] and transport[13] measurements have been carried out on bulk and thin-film samples of $CoSi_2$, $NiSi_2$, and related silicide compounds. Recently, Newcombe and Lonzarich[14] have observed de Haas–van Alphen oscillations in a high-quality $CoSi_2$ sample. This provides an important opportunity to assess the accuracy of present state-of-the-art band-structure methods and local-density theory in determining the electronic properties of this technologically interesting material.

There have been several previous calculations of the $NiSi_2$ band structure[10,15] and density of states[10,15–17] which are found to be in reasonable agreement with the photoemission data.[10–12] The density-of-states results of Tersoff and Hamann[17] for $CoSi_2$ and $NiSi_2$, derived from linear augmented-plane-wave (LAPW) calculations, predict a similar band structure for $CoSi_2$ except that the $3d$-band binding energy is reduced by ~ 2 eV, in accord with photoemission data.[12] Significantly different energy-band results for $CoSi_2$ have been obtained recently by Gupta and Chatterjee[18] using a composite-wave variational version of the APW method. In particular, these results predict a total valence-band width (~ 21.3 eV) which is $\sim 60\%$ larger than the Tersoff-Hamann result.

In order to provide a more complete picture of the $CoSi_2$ band structure, Fermi surface, and related electronic properties, a scalar-relativistic LAPW calculation[19] has been carried out for the fluorite ($C1$) phase of this compound using the observed[20] lattice parameter, $a = 5.356$ Å. The calculations assume nearly touching muffin-tin (MT) spheres which are centered at the Co and Si sites with radii $R(\text{Co}) \approx 2.34$ a.u. and $R(\text{Si}) \approx 2.02$ a.u., respectively. The basis functions included plane waves with energies below 10 Ry (approximately 140 LAPW's). All terms through $l = 6$ have been included in the lattice-harmonic expansion of the nonspherical contributions to the charge density and potential within the MT spheres. The corresponding Fourier expansions in the interstitial region contained about 2500 plane waves. The Brillouin-zone sampling included 28 k points in the $\frac{1}{48}$ irreducible wedge of the full zone. Exchange and correlation effects have been treated using the Wigner interpolation formula.[21]

The LAPW results for $CoSi_2$ are plotted along symmetry lines of the fcc Brillouin zone in Fig. 1. They consist of broad low-lying Si $3s$-$3p$ bands which merge with the relatively narrow Co $3d$ bands just below E_F. The open circles at symmetry points in Fig. 1 identify those states with predominant $3d$ character within the Co MT spheres. Though there is some evidence of broadening due to hybridization effects, the principal Co $3d$-band contribution to the density of states is expected to occur in the energy range 1–3 eV below E_F, in agreement with previous results.[17]

The $CoSi_2$ Fermi level cuts through a hybrid portion of the band structure where the broad $3s$-$3p$ bands are beginning to reemerge. The resulting Fermi surface is relatively simple, consisting of three nested hole pockets that are located at the Brillouin-zone center Γ. These are labeled h_7, h_8, and h_9 since they represent holes in the seventh, eighth, and ninth bands, respectively. The intersection of these three Fermi-surface sheets with the (001) and (110) symmetry planes is shown in Fig. 2. As indicat-

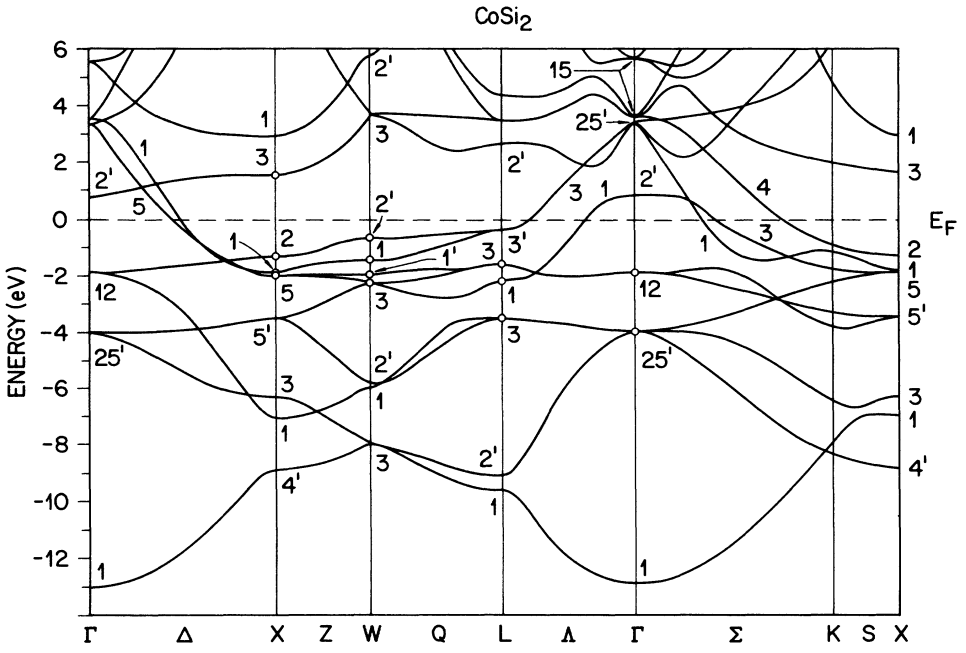

FIG. 1. LAPW energy-band results for $CoSi_2$.

ed, symmetry-induced band degeneracies (Δ_5 and Λ_3) along the $\Delta(\Gamma X)$ and $\Lambda(\Gamma L)$ lines cause the h_7-h_8 and h_8-h_9 surfaces to contact in these directions. Although these degeneracies are removed by spin-orbit effects, the resulting splittings are expected to be small since Co and Si are both light elements with small ($\sim$0.02–0.09 eV) spin-orbit parameters.[22] This leads to the likelihood of magnetic breakdown for orbits that pass near these contacts.

Three-dimensional sketches of the individual h_7, h_8, and h_9 Fermi-surface sheets are shown in Fig. 3. From their shapes, one expects that the extremal orbits which are observed in the de Haas–van Alphen effect will generally involve central orbits (i.e., orbits confined to a plane through the origin). Two exceptions involve h_8 and h_9 when the magnetic field direction **H** is near [001]. For h_8, a pair of noncentral extremal orbits can exist in which the orbit trajectories pass over the four upper and lower [111] bulges. These noncentral orbits enclose an area which is about 15% larger than that of the central orbit when **H** is along [001]. Similar noncentral extremal orbits appear to be possible on the h_9 surface, although this has not been confirmed by means of detailed calculations.

The variation with angle of the central extremal areas and cyclotron masses for orbits on the $CoSi_2$ Fermi surface have been calculated using the Mueller inversion scheme.[23] In this procedure, 19 Fermi radii k_F have been fit (with an accuracy of 1–2%) using an eight-term cubic-harmonic expansion ($l_{max}=14$). The results, which are shown in Fig. 4, have an estimated accuracy of 5 and 15% for the calculated areas and cyclotron masses, respectively. The average (h_7-h_9) calculated cyclotron mass ratio is about 1.0, reflecting the presence of relatively steep bands at E_F in Fig. 1.

As shown by the results summarized in Table I, there is excellent ($\sim$5%) agreement between the calculated and

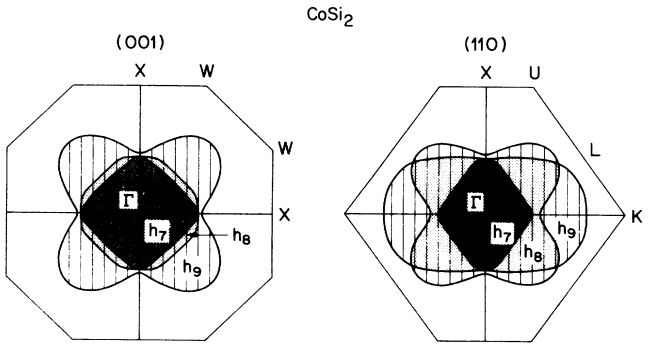

FIG. 2. Calculated central (001) and (110) cross sections of the $CoSi_2$ Fermi-surface sheets h_7, h_8, and h_9.

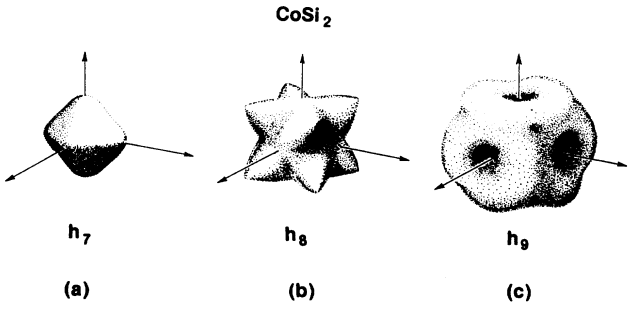

FIG. 3. Three-dimensional sketch of the $CoSi_2$ Fermi-surface sheets h_7 (a), h_8 (b), and h_9 (c).

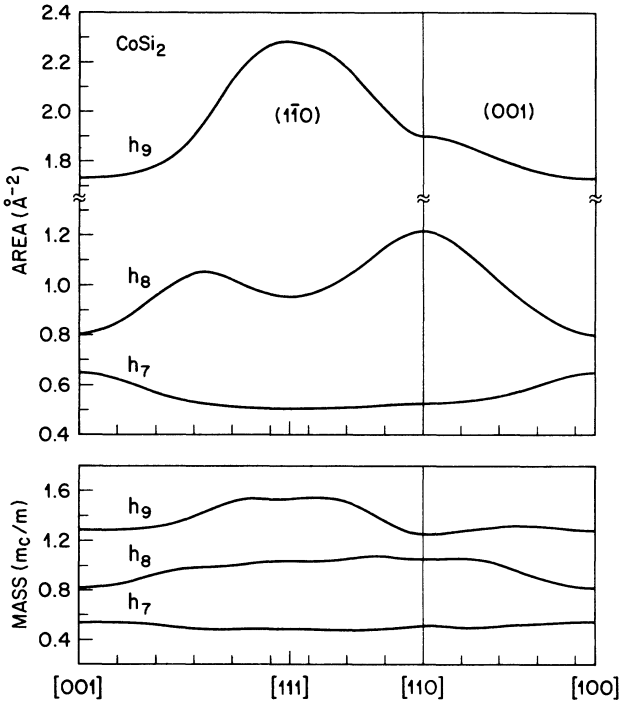

FIG. 4. Calculated central extremal areas and cyclotron masses for magnetic field directions **H** in the (1$\bar{1}$0) and (001) planes.

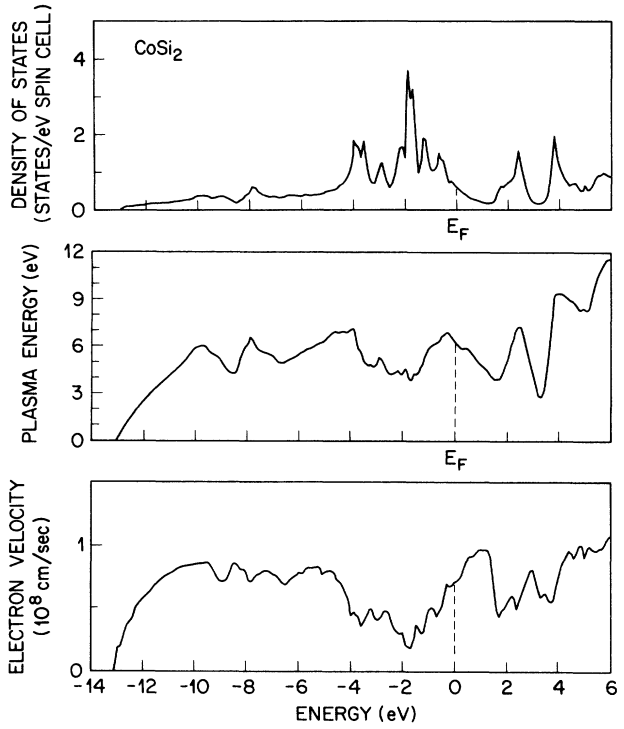

FIG. 5. (a) Calculated density of states, (b) Drude plasma energy, and (c) Fermi velocity for $CoSi_2$.

observed[14] Fermi-surface areas for $CoSi_2$. The larger variations exhibited by the ratio of experimental and calculated cyclotron masses is consistent with the decreased accuracy of the calculated values. This ratio provides an estimate of the electron-phonon coupling parameter $\lambda \sim 0.7 \pm 0.3$ for $CoSi_2$ which is in the range expected for a superconductor with $T_c \approx 1.3$ K (Ref. 24).

The calculated $CoSi_2$ density of states is shown in the top panel of Fig. 5. It has been calculated using tetrahedral interpolation on a mesh of 44 k points in the $\frac{1}{48}$ irreducible Brillouin-zone wedge. It is in good agreement with previous results calculated using a discrete sampling procedure.[17] It agrees equally well with the features exhibited by photoemission data,[12] though the binding energy of the main calculated peak is ~ 0.3 eV larger than the observed value.

The lower panels in Fig. 5 contain the calculated Drude plasma energy $\Omega_p(E)$ and Fermi velocity $v_F(E)$, quantities which are useful for analyzing the transport properties[13] of bulk $CoSi_2$. The calculated carrier density $n = 2.6 \times 10^{22}$ holes/cm^3 is in excellent agreement with Hall data.[13] Combining the calculated values for $\Omega_p(E_F) = 6.2$ eV and $v_F = 0.7 \times 10^8$ cm/sec with the observed low-temperature resistivity $\rho(4\ \text{K}) = 2.6\ \mu\Omega$ cm, one can estimate the mean free path l by use of the relation $l \sim v_F / \Omega_p^2 \rho$ (Ref. 25). The calculated value $l \approx 340$ Å

TABLE I. Comparison of the calculated $CoSi_2$ Fermi-surface areas and cyclotron masses with the de Haas–van Alphen results of Newcombe and Lonzarich (Ref. 14).

		Area (Å^{-2})			Mass (m_c/m)		
H	Sheet	Calc.	Obs.	Ratio	Calc.	Obs.	Ratio
[100]	h_7	0.647	0.655	1.01	0.54	0.78	1.4
	h_8	0.805	0.857	1.06	0.82	1.36	1.7
	h_8	0.923[a]	0.963	1.04		1.34	
	h_9	1.730	1.747	1.01	1.28	2.00	1.6
[110]	h_7	0.524	0.545	1.04	0.51	0.70	1.4
	h_8	1.216	1.230	1.01	1.06	1.55	1.5
	h_9	1.900	1.948	1.03	1.25	2.47	2.0
[111]	h_7	0.503			0.49		
	h_8	0.954			1.03		
	h_9	2.280			1.53		

[a]Noncentral orbit in plane at height $\sim \frac{1}{6}\bar{\Gamma}\,\bar{X}$.

is about a factor of 2 smaller than empirical estimates by Hensel *et al.*[13] that are derived from transport data.

An important consideration in the potential application of $Si/CoSi_2/Si$ heterostructures for use as metal-base transistors concerns the transmission characteristics of the $Si/CoSi_2$ interface. Transmission across a well-ordered epitaxial interface requires that strict kinematical conditions be satisfied. The transmitted state in one material must have the same energy and parallel component of its Bloch wave vector, $\mathbf{k}_{\parallel}$, as the incident state in the other. For the usual case where Si is n type, $\mathbf{k}_{\parallel}$ is determined by the position of the conduction-band minimum along Δ ($\sim 0.85\Gamma X$). Because of band bending at the interface, energy matching involves projected $CoSi_2$ bands at a Schottky-barrier height[3] (~ 0.7 eV) above E_F.

The kinematical conditions for $Si/CoSi_2$ are illustrated in Fig. 6 for three low-index interfaces, (111), (100), and (110). The $CoSi_2$ bands[26] are plotted versus $\mathbf{k}_{\perp}$ for a set of $\mathbf{k}_{\parallel}$ determined by the projections of the Si conduction-band minima on each interface plane. There are six equivalent (0.85,0,0) minima in Si. For the (111) interface, all of these generate equivalent $\mathbf{k}_{\parallel}$, so only one band plot, Fig. 6(a), needs to be considered. Transmission of a Si electron near the conduction-band minimum requires that the dashed line at $E_F+0.7$ eV intersect a $CoSi_2$ band. It does not. We conclude that transmission at this interface requires phonon or impurity scattering to break $\mathbf{k}_{\parallel}$ conservation, or highly excited electrons (~ 0.6 eV) which can reach the first available $CoSi_2$ band.

For the (100) interface, (0.85,0,0) and (0,0,0.85) produce inequivalent $\mathbf{k}_{\parallel}$, and the appropriate band plots for these are shown in Figs. 6(b) and 6(c), respectively. For the (0,0,0.85) case in Fig. 6(c), the kinematical transmission conditions are again unsatisfied. For (0.85,0,0), there appear to be allowed bands. The bands in Fig. 6(b), however, are along the Δ-symmetry line and we must consider the symmetry of the states in each material. From Fig. 1, we see that one of the bands crossing the dashed line has Δ_1 symmetry, which is the same as that of the Si conduction-band states, so that direct transmission is allowed. Finally, for a (110) interface, (0.85,0,0) and (0,0,0.85) are again inequivalent, the bands are not on symmetry lines, and the results in Figs. 6(d) and 6(e) show that transmission is allowed.

We note that satisfying the kinematical conditions does not guarantee a high rate of transmission through an interface. A dynamical calculation of transmission and reflection coefficients is needed for quantitative predictions.

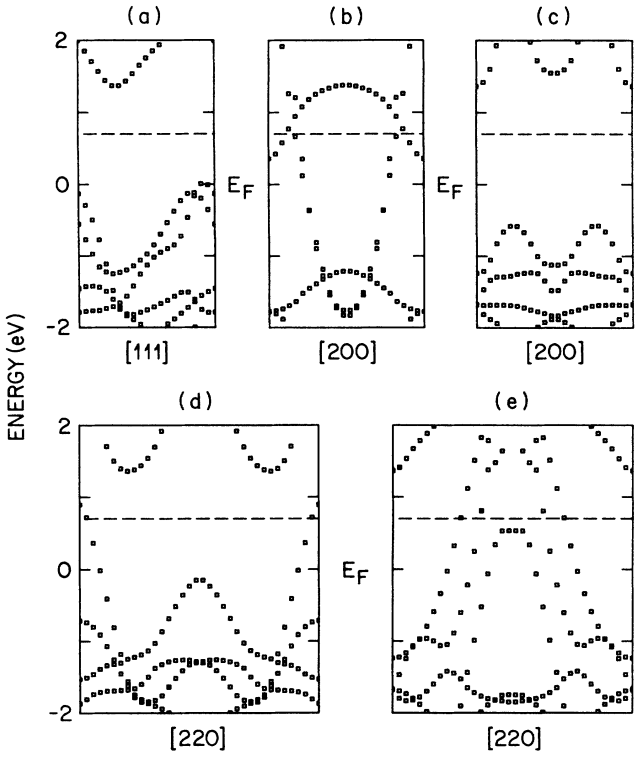

FIG. 6. $CoSi_2$ band plots vs $\mathbf{k}_{\perp}$ for $\mathbf{k}_{\parallel}$ values appropriate for n-type Si and low-index interfaces, as described in the text. The abscissae are $\mathbf{k}_{\perp}$ ranging from 0 to the indicated vector, in units of $(2\pi/a)$.

In conclusion, the results of LAPW calculations for $CoSi_2$ are in good agreement with Fermi-surface and photoemission data. Arguments based on projected bulk bands indicate favorable $Si/CoSi_2$ transmission conditions for (100) and (110) but not (111) interfaces.

The authors are pleased to acknowledge many useful conversations with our colleagues, particularly J. C. Hensel, J. Tersoff, and A. Levi. We are especially grateful to G. C. F. Newcombe for communicating his de Haas–van Alphen results prior to publication.

[1]S. P. Murarka, J. Vac. Sci. Technol. **17**, 775 (1980).
[2]R. T. Tung, J. M. Gibson, and J. M. Poate, Phys. Rev. Lett. **50**, 429 (1983).
[3]R. T. Tung, Phys. Rev. Lett. **52**, 461 (1984); J. Vac. Sci. Technol. B **2**, 465 (1984).
[4]R. J. Hauenstein, T. E. Schlesinger, T. C. McGill, B. D. Hunt, and L. J. Schowalter, Appl. Phys. Lett. **47**, 853 (1985).
[5]E. Rosencher, S. Delage, Y. Campidelli, and F. Arnaud d'Avitaya, Electron. Lett. **20**, 762 (1984).
[6]J. C. Hensel, A. F. J. Levi, R. T. Tung, and J. M. Gibson, Appl. Phys. Lett. **47**, 151 (1985).
[7]E. Rosencher, S. Delage, F. Arnaud d'Avitaya, C. d'Anterroches, K. Belhaddad, and J. C. Pfister, Physica B + C **134B**, 106 (1985).
[8]R. T. Tung, A. F. J. Levi, and J. M. Gibson, Appl. Phys. Lett. **48**, 635 (1986).
[9]E. Rosencher, P. A. Badoz, J. C. Pfister, F. Arnaud d'Avitaya, G. Vincent, and S. Delage, Appl. Phys. Lett. **49**, 271 (1986).
[10]Y. J. Chabal, D. R. Hamann, J. E. Rowe, and M. Schlüter, Phys. Rev. B **25**, 7598 (1982).
[11]Yu-Jeng Chang and J. L. Erskine, Phys. Rev. B **26**, 4766 (1982).

[12]A. Franciosi, J. H. Weaver, and F. A. Schmidt, Phys. Rev. B **26**, 546 (1982); A. Franciosi and J. H. Weaver, Physica B + C **117&118B**, 846 (1983); J. H. Weaver, A. Franciosi, and V. L. Moruzzi, Phys. Rev. B **29**, 3293 (1984).

[13]J. C. Hensel, R. T. Tung, J. M. Poate, and F. C. Unterwald, Appl. Phys. Lett. **44**, 913 (1983); J. C. Hensel, Mater. Res. Soc. Symp. Proc. **54**, 499 (1986).

[14]G. C. F. Newcombe and G. G. Lonzarich, preceding paper, Phys. Rev. B **37**, 10 619 (1988).

[15]D. M. Bylander, L. Kleinman, K. Mednick, and W. R. Grise, Phys. Rev. B **26**, 6379 (1982).

[16]O. Bisi and C. Calandra, J. Phys. C **14**, 5479 (1981); O. Bisi, L. W. Chiao, and K. N. Tu, Phys. Rev. B **30**, 4664 (1984).

[17]J. Tersoff and D. R. Hamann, Phys. Rev. B **28**, 1168 (1983).

[18]R. Sen Gupta and S. Chatterjee, J. Phys. F **16**, 733 (1986).

[19]L. F. Mattheiss and D. R. Hamann, Phys. Rev. B **33**, 823 (1986).

[20]R. W. G. Wyckoff, *Crystal Structures,* 2nd ed. (Krieger, Malabar, Florida, 1982), Vol. 1.

[21]E. Wigner, Phys. Rev. **46**, 1002 (1934).

[22]F. Herman and S. Skillman, *Atomic Structure Calculations* (Prentice-Hall, Englewood Cliffs, New Jersey, 1963).

[23]F. M. Mueller, Phys. Rev. **148**, 636 (1966); L. F. Mattheiss, Phys. Rev. B **1**, 373 (1970).

[24]B. T. Matthias, Phys. Rev. **87**, 380 (1952).

[25]L. F. Mattheiss and L. R. Testardi, Phys. Rev. B **20**, 2196 (1979).

[26]The bands in Fig. 6 were recalculated with the lattice constant of $CoSi_2$ set equal to that of Si, a 1.2% compression.

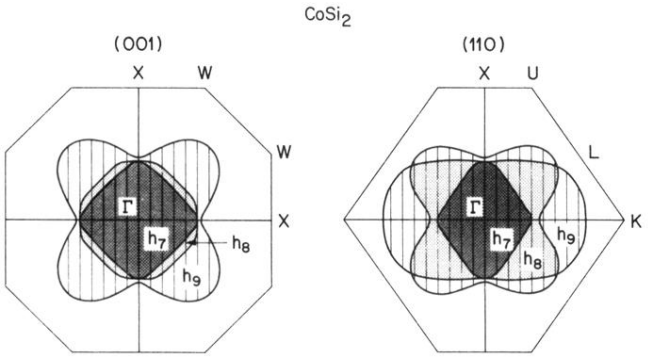

FIG. 2. Calculated central (001) and (110) cross sections of the $CoSi_2$ Fermi-surface sheets h_7, h_8, and h_9.

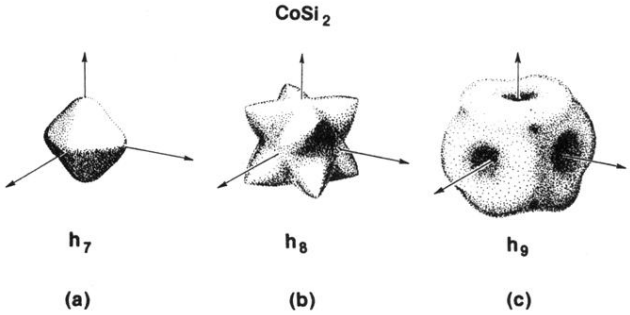

FIG. 3. Three-dimensional sketch of the $CoSi_2$ Fermi-surface sheets h_7 (a), h_8 (b), and h_9 (c).